

Charge carrier mobility in regioregular poly(3-hexylthiophene) probed by transient conductivity techniques: A comparative study

Attila J. Mozer,^{1,*} Niyazi Serdar Sariciftci,¹ Almantas Pivrikas,² Ronald Österbacka,² Gytis Juška,³ Lutz Brassat,⁴ and Heinz Bässler⁵

¹*Linz Institute for Organic Solar Cells (LIOS), Physical Chemistry, Johannes Kepler University Linz, Altenbergerstr. 69, A-4040 Linz, Austria*

²*Department of Physics, Åbo Akademi University, Porthansgatan 3, FIN-20500 Turku, Finland*

³*Department of Solid State Electronics, Vilnius University, Saulėtekio 9, LT-01513, Vilnius, Lithuania*

⁴*H. C. Starck GmbH, Research and Development, Building B 202, D-51368 Leverkusen, Germany*

⁵*Institut für Physikalische-, Kern- und Makromolekulare Chemie, Philipps-Universität Marburg, Hans-Meerwein-Strasse, D-35032 Marburg, Germany*

(Received 16 June 2004; revised manuscript received 13 September 2004; published 27 January 2005)

The temperature and electric-field dependence of charge carrier mobility has been studied by a conventional time-of-flight technique in chemically purified, low dark conductivity samples of regioregular poly(3-hexylthiophene). Subsequently, the mobility of doping-induced charge carriers has been determined using the technique of charge carrier extraction by linearly increasing voltage in the same samples exposed to air. The charge carrier mobility determined by both experimental techniques correspond well to each other at temperatures above 130 K, indicating that these experimental techniques are mutually consistent. The study clearly shows that the typical $\log \mu \propto \beta E^{1/2}$, $\beta > 0$ Poole–Frenkel-like electric-field dependence of the charge carrier mobility diminishes at temperatures around 250–270 K, and β becomes negative at higher temperatures. Such negative electric-field dependence of mobility observed by both experimental techniques is attributed to positional disorder in a random-organic dielectric and analyzed in the framework of the disorder formalism. Finally, the overall agreement indicates that the mode of charge generation has negligible effect on the temperature- and electric-field dependence of mobility except at the lowest temperatures (< 110 K), where transit time dispersion of the photogenerated charge carriers probed by the ToF technique is more pronounced.

DOI: 10.1103/PhysRevB.71.035214

PACS number(s): 72.40.+w, 72.20.-i, 73.50.Dn, 73.61.Ph

I. INTRODUCTION

The determination of the intrinsic charge transport properties of disordered organic semiconductors is important toward developing optoelectronic devices. Charge carrier mobility in organic materials is often measured by the time-of-flight (ToF) technique in which the transit time (t_{tr}) of a sheet of charge carriers, flash photogenerated in a thin, initial region of the sample, is measured in a transient experiment.¹ The mobility is then calculated according to $\mu = d^2 / (V \times t_{tr})$, where d is the sample thickness and V is the applied voltage. The ToF method in disordered materials is limited to moderate electric fields, representative values ranging between 4×10^4 V cm⁻¹ up to 10^6 V cm⁻¹, and to higher temperatures, when the signals are nondispersive. Typical nondispersive and dispersive photocurrent transients are schematically illustrated in Figs. 1(a) and 1(b), respectively. Dispersive transport is often manifested in the absence of a plateau region in the recorded photocurrent transients, in which cases the transit time of charge carriers (t_{tr}) is defined as the intersect of the asymptotes in logarithm photocurrent versus logarithm time plots (see Fig. 1(b)).² Dispersive photocurrent transients are the signature of the absence of quasiequilibrium, i.e., that the relaxation of the photogenerated charge carriers generated initially with random energies toward quasiequilibrium is not completed prior to their arrival at the exit electrode.³ Calculation for disordered semiconductors

showed that the energy of an assembly of charge carriers generated randomly within a localized density of states described by a Gaussian distribution function tends to relax toward the tail states and reach quasiequilibrium with an energy offset of $\langle \epsilon_{\infty} \rangle = -\sigma^2 / kT$ below the center of the distribution.⁴ The time to reach this quasiequilibrium level is increasing faster (as $t_{rel} / t_0 = 10 \exp[-(1.07\sigma/kT)^2]$, where t_0 is the dwell time of a carrier without disorder) than the transit time (t_{tr}) of the charge carriers across the sample; therefore, a crossover from nondispersive to dispersive transport ($ND \rightarrow D$) at lower temperatures is expected.⁴ The displacement of the occupational DOS from the center of the DOS distribution is increasing at lower temperatures; therefore, the temperature dependence of mobility under quasiequilibrium conditions is predicted to be non-Arrhenius type according Eq. (1):⁴

$$\mu(T, E) = \mu_0 \exp \left[-\frac{2}{3} \left(\frac{\sigma}{kT} \right)^2 \right] \exp \left\{ C \left[\left(\frac{\sigma}{kT} \right)^2 - \Sigma^2 \right] E^{1/2} \right\}, \quad (1)$$

where σ [eV] is the width of the Gaussian density of states, Σ is a parameter characterizing positional disorder, μ_0 [cm² V⁻¹ s⁻¹] is a prefactor mobility in the energetically disorder-free system, E [V cm⁻¹] is the electric field, and C is a fit parameter. Temperature dependence according to

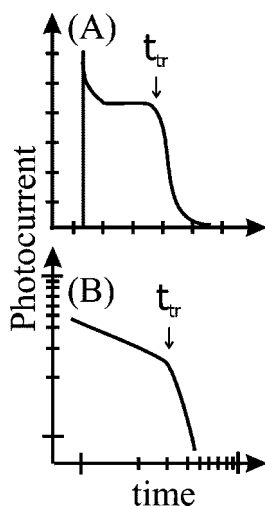


FIG. 1. Schematic of typical (a) nondispersive (b) dispersive photocurrent transients, and the definition of charge carrier transit time (t_{tr}).

Eq. (1) was experimentally observed in various amorphous materials, such as molecularly doped polymers,⁵ molecular glasses,⁶ and conjugated polymers.⁷ Nevertheless, temperature dependence weaker than predicted by Eq. (1) has also been reported,⁸ and has been attributed to the dispersive nature of the charge transport at low temperatures, namely, to the occurrence of an $ND \rightarrow D$ transition.⁹ The temperature at which the transition (T_c) occurs has been found to depend on the energetic disorder parameter, and exhibit sample thickness dependence according to

$$\left(\frac{\sigma}{kT_c}\right)^2 = 44.8 + 6.7 \log d, \quad (2)$$

where d is a parameter related to the thickness (in cm units). The $ND \rightarrow D$ transition is manifested by the appearance of a kink in the $\log \mu (E=0)$ versus $1/T^2$ plots accompanied by photocurrent transients that no longer exhibit a plateau [see Fig. 1(b)].

An alternative explanation to the observed low-temperature behavior has been recently introduced. It was argued that even small concentration of traps can sufficiently pin the transport level at low temperatures resulting in higher mobility values than predicted by a disorder model assuming the presence of only intrinsic charge transport sites.¹⁰ Unfortunately, charge transport in a Gaussian DOS cannot be cast into simple analytical solutions, but one has to rely on the comparison between simulations and experiments.

In this paper, the temperature and electric-field dependence of mobility in a regioregular poly(3-hexylthiophene) P3HT is studied by the well-established ToF technique and compared to the data obtained by the transient conductivity technique of charge extraction by linearly increasing voltage (CELIV).¹¹ The latter method is frequently used to determine mobility in conductive samples with short dielectric relaxation time (τ_σ), e.g., in microcrystalline silicon,¹² in which materials the application of the time of flight technique tends to yield overestimated mobility values due to redistribution of the electric field prior to the arrival of the charge carriers

at the exit electrode ($t_{tr} > \tau_\sigma$).¹³ The method is based on the application of a triangular-shaped voltage pulse to the sample with at least one blocking contact resulting in the extraction of equilibrium charge carriers. The mobility is then calculated from the time to reach the extraction current maximum.¹¹ The CELIV technique requires sufficient amount of intrinsic charge carriers, a condition that is difficult to meet in typical organic semiconductors because of the large optical bandgap. The recent observation of reversible increase of dark conductivity in poly(3-alkylthiophenes) upon exposure to oxygen¹⁴ and/or moisture,¹⁵ however, provides the opportunity to compare the charge carrier mobility of photogenerated carriers and the doping induced equilibrium charge carriers in the same material.

The paper is organized as follows: After a brief description of the experimental arrangements, the charge carrier mobility of photogenerated charge carriers at various electric fields and temperatures probed by the ToF technique (P3HT samples stored in dry argon atmosphere, low conductivity) is presented and samples obtained from different commercial sources are compared. Next, the analysis of the temperature dependence of the shape of the photocurrent transient follows. After that, the temperature- and electric-field dependence of the mobility of the equilibrium (i.e., doping-induced) charge carriers probed by the CELIV technique (P3HT samples exposed to air) is shown, and finally, the results obtained by these two principally different experimental techniques are compared.

P3HT has been selected because of the recent observation of negative electric-field dependence of mobility studied by the time-of-flight technique.¹⁶ The occurrence of such phenomena is thought to originate from the presence of energetic and positional disorder.¹⁷ It was argued, however, that mobilities that decrease with increasing electric field may originate from an experimental artifact related to the ToF technique.^{18,19} The experiment data presented herein confirms that the occurrence of negative electric-field dependence of mobility is an intrinsic property of the materials studied and can be explained by the presence of both energetic and positional disorder as implied by the disorder formalism. The observed mutual agreement between the temperature dependence of the mobility of equilibrium charge carriers probed by the CELIV technique and excess charge carriers photogenerated by short laser pulses probed by the ToF technique suggests that the mode of charge generation does not alter the intrinsic charge transport properties of the material, at least in this low charge carrier concentration regime. However, at low temperatures, where dispersive transport observed in the ToF photocurrent transients starts dominating, deviations between the two techniques are observed.

II. MATERIALS AND EXPERIMENTAL

A. Materials and sample preparation

Regioregular P3HT (the chemical structure is shown in the inset of Fig. 2) was purchased from Rieke Metals, Inc. (Material 1), which was further purified according to the procedure described in Ref. 20, and H. C. Starck GmbH (Material 2), which was used without further purification. The thin

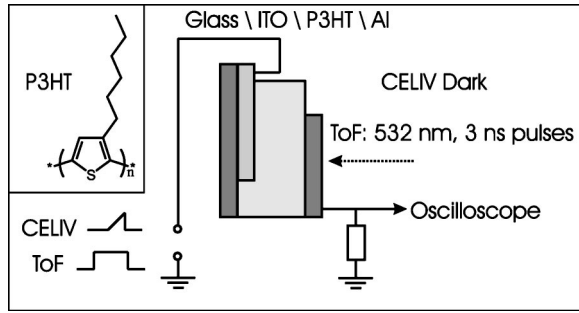


FIG. 2. Experimental setups of ToF and CELIV and the device structure used to measure charge carrier mobility. Inset: Chemical structure of poly(3-hexylthiophene) (P3HT).

films of P3HT were deposited by the doctor-blade technique from chloroform solutions (3 wt % for CELIV samples, 6 wt % for ToF samples) onto structured ITO-coated glass substrates. After preparation, the films were dried in vacuum and transferred to a dry Argon glove box. Aluminum as top electrode was deposited in a vacuum better than 10^{-5} mbar without exposing the devices to air. The thickness of the films was determined using a Tencor Instruments Alphastep Semiconductor Profiler. Figure 2 illustrates the device structure and the experimental setup used to determine the ToF and CELIV mobility.

B. Time-of-flight technique (ToF)

The devices for the ToF technique were transferred into a temperature-controlled liquid-nitrogen-cooled cryostat and kept in vacuum better than 10^{-6} mbar for several hours to remove residual oxygen and moisture. The CELIV curve of such devices showed no extraction of equilibrium charge carriers indicative of very low concentration of equilibrium charge carriers in the dark. The devices were illuminated from the Al side using the second harmonic (532 nm) of a Nd:YAG pulsed laser with 3 ns pulse durations. The photo-generated charges drifted through the sample under the external electric field applied by a voltage supply and were recorded by a digitizing oscilloscope using a low-noise current amplifier. The devices were kept under the constant applied bias between the light pulses to ensure extraction of all the photogenerated carriers between the measurements. The transit time of charge carriers was defined as the intersection point of the asymptotes of the two linear regimes in the double logarithm of photocurrent versus time plots as schematically illustrated in Fig. 1(b). The incident-light intensity was adjusted by optical density filters; the total number of photogenerated charges was less than 10% of the total capacitor charge. The time-of-flight mobility was calculated as $\mu = d^2 / (V \times t_{tr})$, where μ in $\text{cm}^2 \text{V}^{-1} \text{s}^{-1}$ units is the mobility, d is the film thickness, V is the applied potential, and t_{tr} is the transit time of charge carriers.

C. CELIV technique

After preparation, the devices were exposed to air for a few hours to increase conductivity. Subsequently, they were

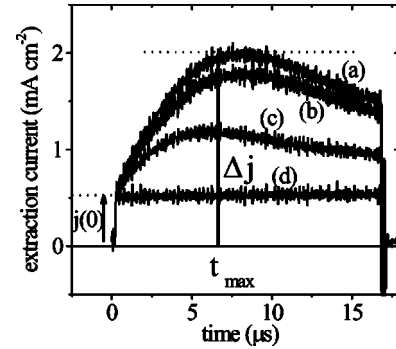


FIG. 3. Recorded CELIV curves upon treatment: (a) at 300 K, shortly after evacuation (b) after 10 min under 10^{-5} mbar pressure, (c) at 340 K after 5 min, (d) at 340 K after 10 min. The voltage rise speed was $10 \text{ V} / 16,66 \mu\text{s}$.

placed into the cryostat, evacuated to 10^{-3} mbar, and disconnected from the vacuum pump. A triangular-shaped reverse bias (ITO connected to the negative terminal) voltage pulse with voltage rise speed $A = dU/dt \text{ V s}^{-1}$ was applied by a function generator, and the extraction current transients were recorded by a digitizing oscilloscope using varying load resistance. The thickness of the active layer ($d = 1.3 \mu\text{m}$) was chosen such that the current density at the maximum of charge carrier extraction (Δj) equals to the current step due to the capacitive response of the device [$j(0) = A \times \epsilon \epsilon_0 / d \text{ mA cm}^{-2}$], in which case Eq. (3) can be applied to calculate the CELIV mobility.¹³

$$\mu = \frac{2d^2}{3At_{\max}^2 \left[1 + 0.36 \frac{\Delta j}{j(0)} \right]}, \quad (3)$$

where d cm is the film thickness, t_{\max} s is the time when the extraction current reaches its maximum value $\Delta j \text{ mA cm}^{-2}$. The electric field changes simultaneously during the extraction. It is maximal at the extraction maximum, i.e., at $t = t_{\max}$, and calculated as Eq. (4):¹³

$$E_{t_{\max}} = \frac{A \times t_{\max}}{d}. \quad (4)$$

The electric-field dependence of mobility was determined by varying the maximum of the triangular voltage pulse between 2 and 10 V, while the duration of the pulse was kept constant. The samples were first measured at room temperature, then cooled down to 110 K and measured again at sequential heating steps up to 310 K.

III. RESULTS

A. Reversible doping of regioregular P3HT

A typical CELIV curve after the samples were exposed to air is shown in Fig. 3(a). The conductivity of the sample is proportional to Δj and calculated according to Eq. (5):¹³

$$\sigma_c = \frac{3\epsilon\epsilon_0\Delta j}{2t_{\max}j(0)}. \quad (5)$$

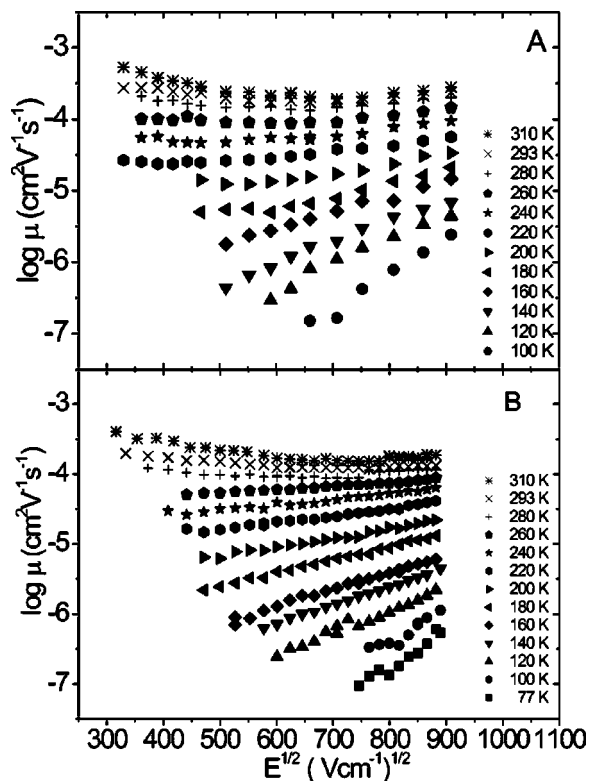


FIG. 4. Electric-field dependence of charge carrier drift mobility at various temperatures measured by the ToF method of (a) Material 1, thickness $d=4.6 \mu\text{m}$ (b) Material 2, thickness $d=3.6 \mu\text{m}$.

The conductivity value of $\sigma_c=1.9 \times 10^{-7} \Omega^{-1} \text{cm}^{-1}$ was calculated shortly after the sample was evacuated, which decreased to $1.7 \times 10^{-7} \Omega^{-1} \text{cm}^{-1}$ 10 min after evacuation [note the smaller Δj in Fig. 3(b)]. The conductivity of the sample decreased faster at elevated temperatures ($\sigma_c = 1.65 \times 10^{-7} \Omega^{-1} \text{cm}^{-1}$ after 5 min at 340 K). The Δj cannot be determined after the devices were kept for ~ 10 min at 340 K, which indicates very low conductivity [Fig. 3(d)]. Figure 3 provides clear evidence that the doping of P3HT is reversible, and related to the influence of volatile dopants, probably oxygen and/or water.

B. Temperature and electric-field dependence of ToF mobility

The temperature- and the electric-field dependence of the mobility determined by ToF technique is shown in Figs. 4(a) and 4(b) for Materials 1 and 2, respectively. For both materials, the slope of the electric-field dependence of mobility is decreasing with increasing temperature, and becomes temperature independent at around 250–270 K. At higher temperatures and at electric field near $2 \times 10^5 \text{V cm}^{-1}$, the $\log \mu(E)$ dependence features a minimum. Such dependence has been observed in molecularly doped polymers²¹ and in a σ conjugated polysilane derivative.²²

Figure 5 shows ToF photocurrent transients obtained for Material 2 and recorded at various applied voltages at 293, 180, and 120 K on logarithm photocurrent logarithm time plots. The transients have been scaled for better comparison. The transit time defined as the intersect of the two linear

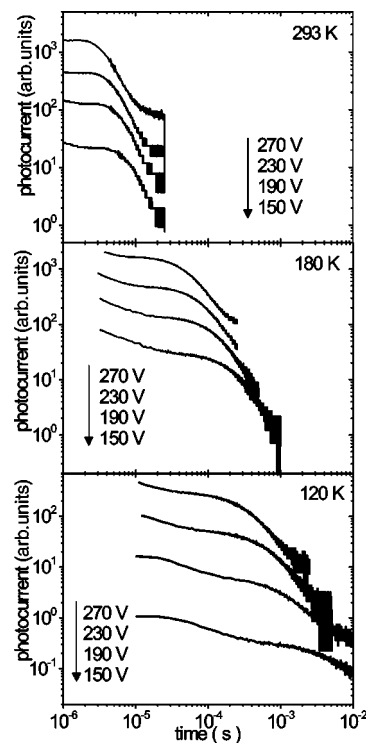


FIG. 5. Recorded ToF photocurrent transients at 293, 180, and 120 K at various applied voltages obtained for Material 2.

regimes is increased by approximately 3 orders of magnitude upon cooling to 120 K. The transit time at each temperature is shorter as the voltage is increased, which shows that the inflection point is clearly related to the charge carrier drift mobility. The photocurrent transients are nondispersive at room temperature as evidenced by the existence of a well-developed plateau and rather short posttransit time tail, but gradually become dispersive at lower temperatures.

The shape of the transients is analyzed according to the formalism developed by Scher and Montroll²³ to describe charge transport in disordered media according to Eqs. (6) and (7).

$$j(t) \sim t^{-(1-\alpha_i)}, \quad t < t_{\text{tr}} \quad (6)$$

$$j(t) \sim t^{-(1+\alpha_j)}, \quad t > t_{\text{tr}}, \quad (7)$$

where α is a parameter describing the dispersivity of the transients and t_{tr} is the transit time defined as the intersects of the straight line in a logarithm photocurrent logarithm time plots. The prediction of that formalism is that the slopes prior $(1-\alpha_i)$ and after $(1+\alpha_j)$ the transit time should sum up to 2, and the transients recorded at various electric fields and thicknesses can be superimposed when normalized to t_{tr} . However, it was shown that Eqs. (6) and (7) are valid only when the distribution of charge transport sites can be described by an exponential function.²⁴

The calculated values of the slope parameters $(1-\alpha_i)$, $(1+\alpha_j)$ and their sum $(1-\alpha_i)+(1+\alpha_j)$ are plotted versus σ/kT in Fig. 6. It is evident that the sum of the slope parameters deviates from 2. In other words, α calculated prior to and after the transit time is not identical, indicating that the

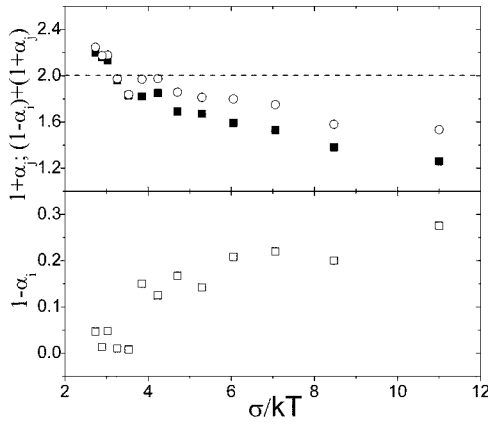


FIG. 6. Temperature (σ/kT) dependence of the slope of the photocurrent transients prior (\square): $(1 - \alpha_i)$, and after (\blacksquare): $(1 + \alpha_j)$ the transit time, and their sum (\circ): $(1 - \alpha_i) + (1 + \alpha_j)$ at an electric field $E = 7 \times 10^{-5} \text{ V cm}^{-1}$.

Scher–Montroll formalism is not applicable to describe charge transport in our samples. Nevertheless, the parameters $(1 - \alpha_i)$ and $(1 + \alpha_j)$ can be used to describe the shape of the photocurrent transients in an operational way to delineate the occurrence of dispersion.²⁵ The determined slope parameter $(1 - \alpha_i)$ is nearly 0 at higher temperatures corresponding to nondispersive transients, but increasing with decreasing temperatures and reaches a value of 0.25 at around 180 K, indicating a $ND \rightarrow D$ transition.⁹ The shape of the photocurrent transients recorded for Material 1 showed similar temperature dependence, i.e., a short plateau at higher temperatures, and a nondispersive-to-dispersive transition at lower temperatures.¹⁶

C. Temperature and electric-field dependence of CELIV mobility

Figures 7(a) and 7(b) shows the CELIV curves recorded at 293 K and 130 K, respectively, at various applied voltages. The time when the extraction current reaches its maximum (t_{max}) is changing by 4 orders of magnitude upon cooling from 293 to 130 K. The shift of t_{max} to longer times is the measure of the temperature dependence of the mobility. t_{max} increases as the speed of the voltage rise $A = dU/dt$ decreases, thus indicating the electric field dependence of the mobility. Dispersion in a CELIV transient can be characterized by the half-width of the extraction current to time t_{max} as $t_{1/2}/t_{\text{max}}$.²⁶ The theoretically calculated value of a nondispersive CELIV transient is $t_{1/2}/t_{\text{max}} = 1.2$. This empirical parameter, which describes the shape of the transient (how fast it rises and decays after reaching its maximum value), has been determined for the CELIV transients presented in Fig. 7, and values between 1.6 and 2.5 have been obtained at 293 K, and it is around 2.6 at 130 K, which is considered moderate when compared to other systems (e.g., $\mu\text{c-Si:H}$).¹²

In the presence of strong dispersion, the extraction peak may shift to shorter times, indicating that only the faster carriers are being probed. Calculation of the amount of extracted charge carriers, however, showed that roughly the same number of carriers are being extracted at each mea-

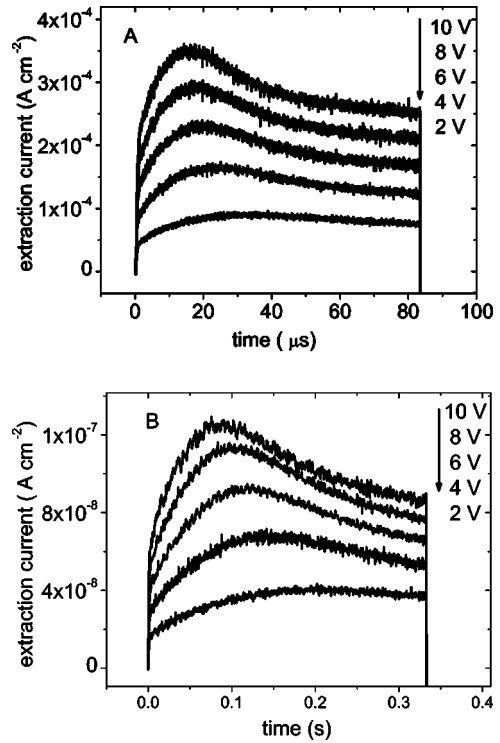


FIG. 7. Recorded CELIV curves in regioregular P3HT samples at (a) 293 K and (b) 130 K. For clarity, the curves shown are for selected applied voltages only.

sured temperature ($\sim n = 3 - 5 \times 10^{14} \text{ cm}^{-3}$), which experimental condition has been chosen by selecting the appropriate frequency of the triangular voltage pulse. In spite of the slightly increased dispersivity of the shape of the CELIV curves at lower temperatures, the t_{max} can be identified and mobility can be calculated in a straightforward manner even at lower temperatures and electric fields.

The mobility was calculated according to Eq. (3), and plotted in Fig. 8 versus squared electric field $[(A \times t_{\text{max}}/d)^{1/2}]$ at various temperatures. The mobility is

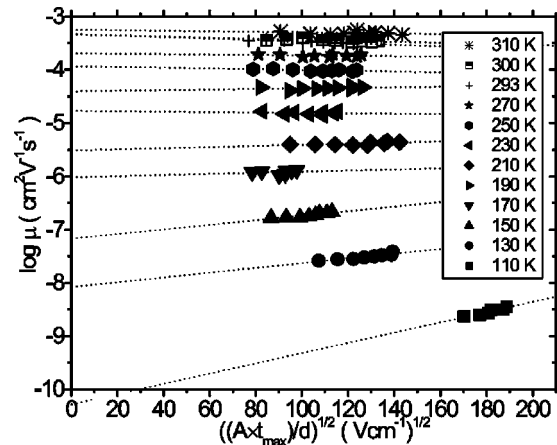


FIG. 8. CELIV mobility values vs square root of electric field calculated according to Eq. (3) at various temperatures. The devices were measured first at 300 K, then cooled to 110 K and measured at subsequent heating steps.

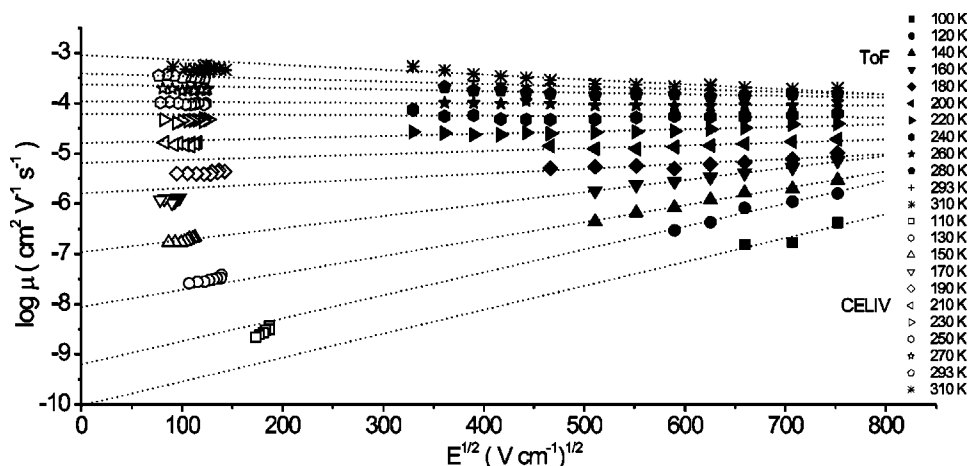


FIG. 9. Temperature- and electric-field dependence of the mobility determined by both time-of-flight (ToF) and CELIV experimental techniques. The dotted lines represent linear fits of the ToF data.

well approximated with a $\log \mu \propto \beta(E)^{1/2}$ electric-field dependence at all measured temperatures. The slope β decreases with temperature, becomes 0 at ~ 250 K, and turns to negative at higher temperatures. The amount of extracted charge carriers calculated from CELIV curves recorded at the beginning of the measurements (300 K) was $n=3 \times 10^{14} \text{ cm}^{-3}$, which is decreased by $\sim 50\%$ toward the end of the experiment (e.g., $n=1.75 \times 10^{14} \text{ cm}^{-3}$ measured at 293 K) due to evaporation of volatile dopants in vacuum as it was demonstrated above. Nevertheless, the mobility value and its electric-field dependence measured at 293 K are not affected by this change as it is shown in Fig. 8.

IV. DISCUSSION

In principle, the CELIV technique probes the mobility of the more mobile charge carriers. If both carriers are mobile, two extraction peaks corresponding to extraction of both carriers may be observed.²⁶ The extraction current in our experiment is dominated by holes rather than electrons due to the orders of magnitude higher mobility of the former. This is confirmed by the ToF technique in which the photocurrent transients of electrons featured a fast exponential decay without clear transit time indicative of efficient electron trapping.²⁷

The temperature and electric-field dependence of the hole mobility obtained by both experimental techniques is plotted in Fig. 9. Note that at lower temperatures, the temperature steps used in the CELIV measurement and ToF were not identical. The dotted lines represent linear fits of the $\log \mu$ versus $E^{1/2}$ plots obtained by the ToF technique. The overall agreement between the experiments shows that the two different experiment techniques are mutually consistent. First, the negative electric-field dependence of mobility observed at higher temperatures will be discussed followed by the discussion of the temperature dependence of the charge carrier mobility.

A. Negative electric-field dependence of mobility

The temperature dependence of the slope of the electric field dependence ($\beta = \delta \log \mu / \delta E^{1/2}$) obtained by the ToF and the CELIV technique is compared in Fig. 10. The electric-

field dependence from the ToF measurements was determined from the lower region of the electric field, i.e., $< 2 \times 10^5 \text{ V cm}^{-1}$. Clearly, the slope of the field dependence measured by both techniques turns to negative for both materials and all samples studied. The strong increase of the field dependence of mobility around 110 K observed by the CELIV technique might be an artifact. The electric field according to Eq. (4) depends on both space and time coordinate; therefore, the electric field may be overestimated in the presence of stronger dispersion at low temperatures. Nevertheless, the overall agreement and, particularly, the occurrence of negative electric field dependence of mobility at higher temperatures, when the transients by both experimental techniques can be characterized as nondispersive, justifies the applicability of Eq. (1) and has the following implications.

It has been proposed that the observation of mobilities that decrease with increasing electric field in poly(3-alkylthiophenes) is an artifact of the ToF technique might be caused by screening of the electric field in conductive samples.¹³ In such cases, the time-of-flight technique yields higher apparent mobility values that strongly increase with decreasing electric field below a critical electric field $E < 4 \times 10^4 \text{ V cm}^{-1}$. Clearly, the rather weak negative electric-field dependence of mobility in Fig. 4 measured by the ToF technique below $< 2 \times 10^5 \text{ V cm}^{-1}$ cannot be attributed to such a spurious electric-field effect. Moreover, such negative electric-field dependence has been observed in several samples with various devices thicknesses (between 3.6 and 6 μm). The experiments presented in this comparative study clearly demonstrate that the negative electric-field dependence of the mobility is confirmed by the CELIV technique, which was shown to yield the correct electric-field dependence in moderately conductive samples.¹⁸

The agreement between the mobility data inferred from both ToF and CELIV also proves that the negative electric-field dependence of mobility observed over a wide electric-field region is not caused by electric-field independent carrier diffusion¹⁹ that may become dominant at electric-fields weaker than $2 \times 10^4 \text{ V cm}^{-1}$. A straightforward experimental check of the effect of diffusion on the transit time and therefore mobility is indeed the application of the CELIV technique, because there is no diffusion current at $t=0$ due to

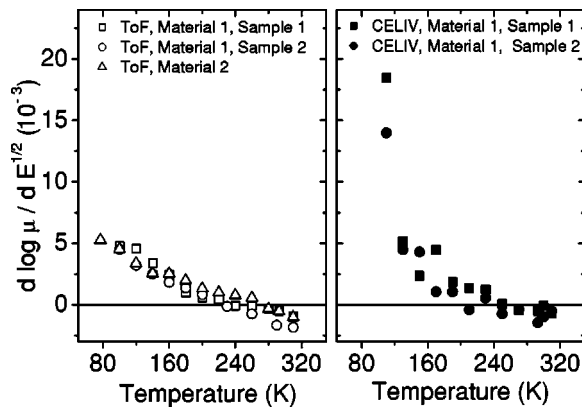


FIG. 10. Slope of the electric-field dependence of mobility versus temperature determined by the ToF technique (empty symbols) and by the CELIV technique (full symbols); for Material 1 and Material 2 with different sample thickness (see Table I).

thermodynamic equilibrium established prior to the application of the voltage pulse. The charge carriers are distributed homogeneously throughout the dielectric prior charge extraction provided that the delay time between subsequent voltage pulses is sufficiently long. In no case was the shape of the extraction transients affected in our experiments when the delay time between the voltage pulses was raised up to 3 s, which confirms that the equilibrium condition was recovered. Furthermore, photocurrent transients due to diffusion are expected to be strongly dispersive, electric-field independent, but dependent on sample thickness. These predictions are in direct contradiction to the experimental observation presented herein.

Disorder Formalism [Eq. (1)] attributes the temperature and electric-field dependence of mobility to two main parameters, namely, energetic and positional disorder. The energetic disorder parameter is related to the width of the Gaussian DOS normalized to kT , and it is mainly responsible for the temperature dependence of mobility. The positional disorder, on the other hand, arises due to fluctuation of the intersite coupling either due to variation of intersite distance between the charge transport sites or simply the variation of overlap between corresponding electronic orbitals. In the absence of positional disorder and under the condition of quasiequilibrium, the motion of a charge carrier in a rough energy landscape is controlled by activated jumps toward sites close to the statistically defined transport energy.¹⁰ The latter is located below the center of the Gaussian density of states distribution (DOS) and decreases weakly with temperature. At weak to moderate electric-fields the diffusive motion and the superimposed drift is in accordance with the Einstein ratio between drift and diffusion. As the field increases, the activation energy is lowered by the drop of the electrostatic potential between two sites relative to kT . Therefore the charge carrier mobility should increase while the diffusive character of motion is still retained. This is no longer the case when, on average, the drop of the electrostatic potential becomes comparable and even exceeds the energy barrier for an along-field jump. In that case the dwell time of a carrier on a site approaches the reciprocal rate for that jump because jumps against the field direction are gradually eliminated.

Accordingly, the transport velocity must saturate with field. This implies a linear decrease of the carrier mobility because it is controlled by energetically downward jumps only that are not accelerated.

The situation is more complex if positional disorder becomes important. In that case a carrier can avoid an energetically unfavorable site by executing a detour around that site. This resembles motion in a percolating cluster and leads to an increase of the overall carrier mobility at moderate fields. However, the interplay between drift and diffusion is field dependent, as it is in the case of pure energetic disorder because the excess motional freedom a carrier gains by following the detour path is gradually eliminated at higher fields. Importantly, however, the critical field for that effect is dictated by the drop of the electrostatic potential across the percolating cluster (i.e., the degree of positional disorder rather than by the intersite distance). This leads to an S -like ($\beta = \delta \log \mu \propto \delta E^{1/2}$) dependence. At very low fields, μ is constant and tends to decrease as the field increases. Eventually, β reverses sign when the additional carrier loops are blocked and the effect of energetic disorder takes over. At highest electric fields, μ decreases again because the transport velocity saturates.

The above qualitative reasoning has been based on a hopping concept involving Miller–Abrahams-type jump rates. However, the phenomenological transport characteristics can similarly be rationalized in terms of Marcus-type jump rates.²⁸ The recent theoretical work by Fishchuk *et al.*²² employing the effective medium approach shows that the shape of the $\mu(E)$ dependence is independent of the choice of the form the rates. Furthermore, the decrease of μ at very low electric-fields can, in principal, be recovered by invoking the inverted Marcus jump regime. However, a detailed analysis of mobility data for a system, where structural site relaxation is important, indicates that unrealistically large value of the reorganization energy are required in order to explain the decreases of the hole mobility at very high electric-fields, while a hopping approach yields reasonable fit parameters.²⁹

B. Temperature dependence of mobility

Another implication of the mutual agreement between the results obtained by the ToF and CELIV relates to the temperature dependence of the mobility. The ToF technique probes the motion of charge carriers generated initially with random energies. Dispersive transport occurs if the mean hopping rate of the charge carriers decreases as the function of time.³⁰ Since the energy relaxation of the charge carriers is faster at higher temperatures, the photocurrent transient settles to a plateau indicating that nondispersive transport is reached prior to the arrival of the charge carriers at the exit electrode. The time to reach quasiequilibrium, however, is increasing faster than the transit time with decreasing temperature; therefore, dispersive transport starts dominating at lower temperatures as indicated by dispersive photocurrent transients. The CELIV method, on the other hand, probes the mobility of doping induced (equilibrium) charge carriers occupying the tail energy states of the DOS without further relaxation.

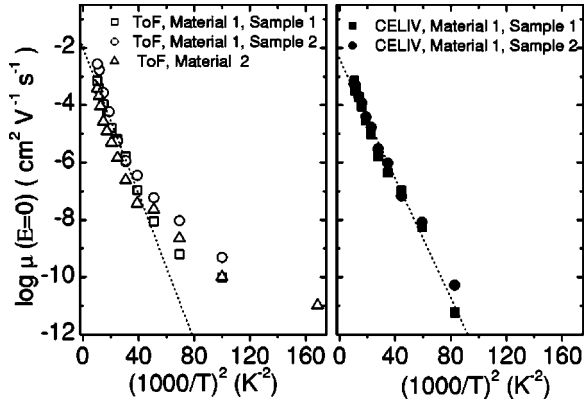


FIG. 11. Temperature dependence of the mobility extrapolated to zero electric field determined by the ToF (empty symbols) and CELIV technique (full symbols) for Materials 1 and 2 with different sample thickness (see Table I).

The mobility values obtained by the ToF and CELIV extrapolated to zero electric-field are plotted versus inverse temperature squared in Fig. 11 according to Eq. (1). Mobility obtained for several samples yield consistent values for $T > 130$ K. The low-temperature ToF mobilities, on the other hand, tend to yield higher values indicating that more mobile carriers are being probed. In a previous paper, it was demonstrated that the determined mobility values also deviate from the prediction of a simple Arrhenius-type activation ($\log \mu \propto 1/T$) at lower temperatures.¹⁶ The observed low-temperature deviations can be explained by the occurrence of an $ND \rightarrow D$ transition as discussed above. The transition temperature (T_c), which marks the $ND \rightarrow D$, is calculated according to Eq. (2), and using the value of $\sigma = 70$ meV calculated from Fig. 11, $T_c = 180$ K is obtained. The calculated value of T_c is consistent with the observed dispersivity of the recorded photocurrent transients below 180 K.

On the other hand, the CELIV values follow the $\log \mu (E=0) \propto T^{-2}$ temperature dependence at all temperatures as predicted by Eq. (1). It should be noted that the lower value of CELIV mobility measured at 110 K may be due to some overestimated electric-field dependence (see the discussion in Sec. IV A).

Dispersive transport has been observed in conjugated polymers probed by impedance spectroscopy³¹ and a transient electroluminescence technique.³² The dispersion was analyzed within the framework of the Scher–Montroll for-

malism, and a temperature-independent dispersion parameter $\alpha = 0.45$ has been calculated and was attributed to the distribution of transit times. The $ND \rightarrow D$ transition discussed here, on the other hand, is intrinsic to the ToF technique, in which the charge carriers are generated under nonequilibrium conditions leading to a mean hopping rate that decreases at longer times.

From linear regression in Fig. 11, parameters μ_0 , σ are calculated, and shown in Table I together with Σ and C calculated from linear fit of the field dependence of mobility versus the energetic disorder parameter $(\sigma/kT)^2$. The zero field mobility values as well as the electric-field dependence obtained by the ToF technique were fitted above 180 K, where the relationship is well approximated by a linear relationship. The calculated values of σ are in good agreement between the measurements, which indicates that the reversible (very weak) doping of P3HT does not alter the density of states distribution significantly, at least in this regime, where the conductivity ($\sim \sigma_c = 10^{-8} \Omega^{-1} \text{cm}^{-1}$) and the carrier concentration ($\sim n = 10^{14} - 10^{15} \text{cm}^{-3}$) is considered to be rather low. Furthermore, the calculated prefactor mobility values agree reasonably well between the two experiments. Considering the principal differences by the two applied methods, this finding suggests that charge carrier motion does not depend on the mode of charge generation in the regioregular P3HT samples under the presented experimental conditions. In accordance with the disorder model, the rather small σ and large Σ obtained by both experimental techniques are thought to be responsible for the observed negative electric-field dependence of mobility.

V. CONCLUSIONS

Two independent methods for charge carrier mobility determination, namely, (a) time of flight (b) charge carrier extraction by linearly increasing voltage (CELIV) have been used in a regioregular poly(3-hexylthiophene). The latter method probes the motion of charges generated by homogeneous doping throughout the bulk, whereas in the ToF method, a sheet of excess carriers generated by a laser flash drifts across the sample. By applying both techniques in the same poly(3-hexylthiophene) with or without doping, it has been shown that the results are mutually consistent except at low temperatures (< 130 K), when strong dispersion of the carrier motion become important. Another fundamental issue

TABLE I. Determined values of μ_0 (prefactor mobility), σ (energetic disorder), C (fit constant), and Σ (positional disorder parameter) of the disorder formalism [Eq. (1)] obtained by CELIV and time-of-flight (ToF) techniques.

| Material/Sample | Method | μ_0 ($\text{cm}^2 \text{V}^{-1} \text{s}^{-1}$) | σ (meV) | C [$(\text{cm V}^{-2})^{1/2}$] | Σ | Thickness (μm) |
|-----------------|------------------|---|----------------|------------------------------------|----------|-----------------------------|
| 1/1 | CELIV | 4×10^{-3} | 63 | 3.6×10^{-4} | 3 | 1.3 |
| 1/2 | CELIV | 4×10^{-3} | 61 | 3.6×10^{-4} | 3.15 | 1.3 |
| 1/1 | ToF ^a | 1×10^{-2} | 70 | 1.5×10^{-4} | 3.4 | 4.6 |
| 1/2 | ToF ^a | 5×10^{-2} | 74 | 2.1×10^{-4} | 3.9 | 6.4 |
| 2/1 | ToF ^a | 5×10^{-3} | 73 | 1.4×10^{-4} | 3 | 3.6 |
| 2/2 | ToF ^a | 7×10^{-3} | 75 | 1.4×10^{-4} | 3 | 6.5 |

^aCalculated between 310–180 K temperature region.

is the observation of the negative electric-field dependence of mobility at moderate electric fields. By applying both techniques, we confirmed that the negative electric-field dependence of mobility is an intrinsic feature of the investigated materials. Large degrees of positional disorder equivalent to the large spread of intersite coupling matrix elements are proposed to be responsible for this negative electric-field dependence of mobility as suggested by the disorder model.

ACKNOWLEDGMENTS

The authors acknowledge the financial support of the European Research and Training Network (RTN) project EUROMAP (Contract No. HPRN-CT-2000-00127), and the support of the Academy of Finland through Grant No. 206110. Heinz Bässler acknowledges financial support of the European Commission in the framework of LAMINATE.

*Email address: attila.mozer@jku.at

- ¹P. M. Borsenberger and D. S. Weiss, *Organic Photoreceptors for Xerography* (Marcel Dekker, Inc., New York, 1998).
- ²H. Scher and E. W. Montroll, *Phys. Rev. B* **12**, 2455 (1975).
- ³D. Hertel, H. Bässler, U. Scherf, and H. H. Hörhold, *J. Chem. Phys.* **110**, 9214 (1999).
- ⁴H. Bässler, *Phys. Status Solidi B* **175**, 15 (1993).
- ⁵P. M. Borsenberger and J. J. Fitzgerald, *J. Phys. Chem.* **97**, 4815 (1993).
- ⁶Y. Shirota, *J. Mater. Chem.* **10**, 1 (2000).
- ⁷H. C. F. Martens, P. W. M. Blom, and H. F. M. Schoo, *Phys. Rev. B* **61**, 7489 (2000); A. J. Mozer, P. Denk, M. C. Scharber, H. Neugebauer, N. S. Sariciftci, P. Wagner, L. Lutsen, and D. Vanderzande, *J. Phys. Chem. B* **108**, 5235 (2004).
- ⁸C. Im, H. Bässler, H. Rost, and H. H. Hörhold, *J. Chem. Phys.* **113**, 3802 (2000); P. M. Borsenberger, L. T. Pautmeier, and H. Bässler, *Phys. Rev. B* **46**, 12 145 (1992).
- ⁹P. M. Borsenberger, R. Richert, and H. Bässler, *Phys. Rev. B* **47**, 4289 (1993).
- ¹⁰V. I. Arkhipov, P. Heremans, E. V. Emelianova, G. J. Adriaenssens, and H. Bässler, *J. Phys.: Condens. Matter* **14**, 9899 (2002).
- ¹¹G. Juška, K. Arlauskas, M. Viliunas, and J. Kočka, *Phys. Rev. Lett.* **84**, 4946 (2000).
- ¹²G. Juška, N. Nekrasas, K. Genevičius, J. Stuchlik, and J. Kočka, *Thin Solid Films* **451–452**, 290 (2004).
- ¹³G. Juška, K. Arlauskas, M. Viliunas, K. Genevičius, R. Österbacka, and H. Stubb, *Phys. Rev. B* **62**, R16 235 (2000).
- ¹⁴Z. Bao, A. Dodabalapur, and A. J. Lovinger, *Appl. Phys. Lett.* **69**, 4108 (1996); M. S. A. Abdou, F. P. Orfino, Z. W. Xie, M. J. Deen, and S. Holdcroft, *Adv. Mater. (Weinheim, Ger.)* **6**, 838 (1994).
- ¹⁵S. Hoshino, M. Yoshida, S. Uemura, T. Kodzasa, N. Takada, T. Kamata, and K. Yase, *J. Appl. Phys.* **95**, 5088 (2004).
- ¹⁶A. J. Mozer and N. S. Sariciftci, *Chem. Phys. Lett.* **389**, 438 (2004).
- ¹⁷P. M. Borsenberger, *J. Appl. Phys.* **68**, 5682 (1990).
- ¹⁸G. Juška, K. Genevičius, K. Arlauskas, R. Österbacka, and H. Stubb, *Phys. Rev. B* **65**, 233208 (2002).
- ¹⁹H. Cordes, S. D. Baranovskii, K. Kohary, P. Thomas, S. Yamasaki, F. Hensel, and J.-H. Wendorff, *Phys. Rev. B* **63**, 094201 (2001); A. Hirao, H. Nishizawa, and M. Sugiuchi, *Phys. Rev. Lett.* **75**, 1787 (1995).
- ²⁰M. M. Erwin, J. McBride, A. V. Kadavanich, and S. J. Rosenthal, *Thin Solid Films* **409**, 198 (2002).
- ²¹A. Peled and L. B. Schein, *Chem. Phys. Lett.* **153**, 422 (1988); M. Novo, M. van der Auweraer, F. C. DeSchryver, P. M. Borsenberger, and H. Bässler, *Phys. Status Solidi B* **177**, 223 (1993).
- ²²I. I. Fishchuk, A. Kadeshchuk, H. Bässler, and M. Abkowitz, *Phys. Rev. B* **70**, 245212 (2004).
- ²³H. Scher, M. F. Shlesinger, and J. T. Bendler, *Phys. Today* **44**, 26 (1991).
- ²⁴V. I. Akhipov and A. I. Rudenko, *Philos. Mag. B* **45**, 18 (1982).
- ²⁵P. M. Borsenberger, L. T. Pautmeier, and H. Bässler, *Phys. Rev. B* **46**, 12 145 (1992).
- ²⁶G. Juška, N. Nekrasas, K. Arlauskas, J. Stuchlik, A. Fejfar, and J. Kočka, *J. Non-Cryst. Solids* **338–340**, 353 (2004).
- ²⁷S. S. Pandey, W. Takashima, S. Nagamatsu, T. Endo, M. Rikukawa, and K. Kaneto, *Jpn. J. Appl. Phys., Part 2* **39**, L94 (2000).
- ²⁸R. A. Marcus, *Rev. Mod. Phys.* **65**, 599 (1993).
- ²⁹B. Hartenstein, H. Bässler, S. Heun, P. Borsenberger, M. van der Auweraer, and F. C. DeSchryver, *Chem. Phys.* **191**, 321 (1995).
- ³⁰L. Pautmeier, R. Richert, and H. Bässler, *Philos. Mag. Lett.* **59**, 325 (1989).
- ³¹H. C. F. Martens, H. B. Brom, and P. W. M. Blom, *Phys. Rev. B* **60**, R8489 (1999).
- ³²P. W. M. Blom and M. C. J. M. Vissenberg, *Phys. Rev. Lett.* **80**, 3819 (1998).